https://doi.org/10.15407/ujpe68.11.750

A. JUMABAEV,[1,2] A.A. ABSANOV,[1] H.A. HUSHVAKTOV,[1] L.A. BULAVIN[3]

[1] Sharof Rashidov Samarkand State University
(15, University Blvd., Samarkand 703004, Uzbekistan; e-mail: jumabaev2@rambler.ru)
[2] Uzbek–Finnish Pedagogical Institute
(166, Spitamen Ave., Samarkand 703004, Uzbekistan)
[3] Taras Shevchenko National University of Kyiv
(64/13, Volodymyrska Str., Kyiv 01601, Ukraine)

INTERMOLECULAR INTERACTIONS IN LIQUID PROPIONIC ACID AND ITS SOLUTIONS: RAMAN AND DFT STUDIES

The mechanism of molecular complex formation in liquid propionic acid and its solutions is investigated. The anisotropic component of the Raman band of the C=O stretching vibration of pure propionic acid consists of three bands with maxima at 1661, 1700, and 1753 cm^{-1}. The effect of varying the concentrations of solvents such as CCl_4, acetonitrile, and water on this vibration mode is studied. The mechanism of formation of molecular complexes in solutions is determined using DFT calculations at the B3LYP/6-311++G(d,p) level of theory. The AIM, RDG, and NCI topological analyses are also performed to investigate the intermolecular interactions in the complexes.

Keywords: propionic acid, Raman spectroscopy, DFT, intermolecular interactions.

1. Introduction

Molecular complexes of carboxylic acids in the liquid phase have attracted the attention of researchers for a long time [1–6]. Their formation is usually manifested in Raman and IR spectra, especially in the spectral region of C=O and O–H vibrations [4]. The structure of the most common molecular complex in carboxylic acids is a dimer formed due to the intermolecular hydrogen bonding between two carboxyl groups, and it mainly has a cyclic structure with a local inversion center [7–10]. The study of the structure and vibrational characteristics of such hydrogen-bonded complexes is the main subject of experimental and theoretical researches [11–14]. In addition to their biological and medicinal properties, the studies of homo- and hetero-complexes of carboxylic acids in gaseous, liquid, and solid states provide information on the nature of non-covalent interactions, including the O–H···O=C interaction.

The results of studies of simple carboxylic acids, such as formic acid dimer species involved in strong and weak intermolecular interactions, have recently been published in [15–18]. Based on the computed vibrational spectra of monomers and O–H···O-bonded dimer species, Karabacak *et al.* [19] identified IR and Raman modes of solid isophthalic acid. Taylor *et al.* [20] published *ab initio* predictions of the effects of the temperature and solvation on the dimerization of benzoic acid molecules. According to their findings, between benzoic acid molecules, the strong H-bonds are formed in a variety of complexes, but the cyclic dimer is the most stable of them. Using Monte Carlo and molecular dynamics (MD) simulations, Marcinovic *et al.* proposed a self-assembly model of butanedioic acid [21]. Other authors describe ordered cyclic structures stabilized by two O–H···O bonds between the two carboxylic groups in their structural analyses of isophthalic acid and 5-fluoroisophthalic acid [22–24].

According to the literature review, the molecular structure and intermolecular interactions in propionic acid (PA) in the liquid phase have not been thoroughly explored. In this study, we will investi-

Citation: Jumabaev A., Absanov A.A., Hushvaktov H.A., Bulavin L.A. Intermolecular interactions in liquid propionic acid and its solutions: Raman and DFT study. *Ukr. J. Phys.* **68**, No. 11, 750 (2023). https://doi.org/10.15407/ujpe68.11.750.

Цитування: Жумабаєв А., Абсанов А.А., Хушвактов Х.А., Булавін Л.А. Міжмолекулярні взаємодії в рідкій пропіоновій кислоті та її розчинах: дослідження за допомогою раманівської спектроскопії та теорії функціонала густини. *Укр. фіз. журн.* **68**, №11, 752 (2023).

gate the effect of solvents such as CCl_4, acetonitrile, and water on the polarized and unpolarized Raman spectra of liquid propionic acid. The C=O stretching vibration was chosen for such studies, since it is rather isolated from other vibrational modes [25, 26]. Quantum-chemical calculations were performed at the B3LYP/6-311++G(d,p) level using the DFT approach to investigate the mechanism of intermolecular interactions and the formation of molecular complexes in pure propionic acid and its different solutions. In addition, we analyze the charge distribution in H-bonded molecular complexes by Atoms in Molecules (AIM), Reduced Density Gradient (RDG), and Non-Covalent Interaction (NCI) analyses.

2. Methods

2.1. Experimental Method

A DFS-52 spectrometer was used to record the Raman spectra of liquid propionic acid and its solutions with carbon tetrachloride, water, and acetonitrile at a temperature of 252 °C. As an excitation light source, an argon ion laser LGN-503 (488 nm, 1 W) was used. All measurements were made with polarized light in the 90° scattering geometry. A polarizing prism selects the polarized constituents of the scattered light. Chemically pure substances were used in the experiment, which were also subjected to a further distillation under vacuum. The spectral gap width was 1.8 cm^{-1} in all measurements. Errors in determining the relative position of the maximum and half-width of the spectral bands were 0.3 cm^{-1}. The errors in calculating the relative position of the spectral bands' maxima and half-widths were 0.3 cm^{-1}. All solutions were prepared in accordance to the molar fractions of the components.

2.2. Computational details

All calculations were carried out in the Gaussian 09W programme [27] using the Density Functional Theory (DFT) method. To account for intermolecular hydrogen bonding, calculations were carried out using the B3LYP functional and the 6-311++G(d,p) basis set, which included the diffusion and polarization functions. In addition, the calculations, where propionic acid, acetonitrile, and water were considered as envoronments, were performed using the integral equation formalism polarized continuum model (IEF-PCM) to account for the effect of the solution as accurately as possible.

Atoms in Molecules (AIM), Reduced Density Gradient (RDG), and Non-Covalent Interaction (NCI) topological analyzes based on Bader's theory [28] were performed to further study the non-covalent interactions between molecules [43–45]. Topological parameters were calculated using the MultiWfn software [29] and visualized using the VMD software [30].

3. Results and Discussions

3.1. Raman spectra analysis

The polarized Raman spectra of pure propionic acid and its solutions in CCl_4 with concentrations ranging from 0.1 to 0.7 were recorded. It is known that the shape of isotropic and anisotropic components of Raman bands is determined by intermolecular interactions. The intensities of isotropic and anisotropic components can be calculated using the following equations [31]:

$$I_{\text{iso}}(\nu) = I_{\perp}(\nu) - \frac{4}{3} I_{\parallel}(\nu),$$
$$I_{\text{aniso}}(\nu) = I_{\parallel}(\nu),$$

where $I_{\perp}(\nu)$ and $I_{\parallel}(\nu)$ are the experimentally measured polarized (perpendicular) and depolarized (parallel) components of the Raman intensity.

Figure 1 shows the anisotropic (parallel) components of the Raman band of the C=O stretching vibration of propionic acid. It can be seen from the figure that the parallel component of the C=O vibration band of pure liquid PA consists of three broad bands with maxima at 1661, 1700, and 1753 cm^{-1}. Similarly, these three bands are observed in the perpendicular component. The ratios of intensities for the parallel and perpendicular components of these bands are different. This means that the depolarization coefficients of the bands also have different values. The band at 1753 cm^{-1} has the highest value of the depolarization ratio. The depolarization ratio of the 1700 cm^{-1} band is much lower, and the depolarization coefficient of the 1661 cm^{-1} band is even lower. In [32], it was shown that C=O vibrational bands of acetic and trifluoroacetic acids also consist of three bands, corresponding to different associates. Similarly, one can suppose that the splitting of this band in PA has the same nature.

The frequency of the C=O stretching vibration is determined by the distribution of the electron cloud along the C=O bond. The change of this distribution after the formation of the H-bond between molecules

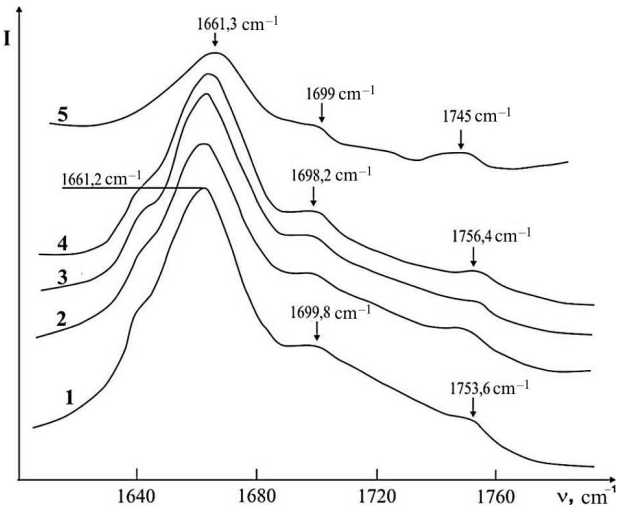

Fig. 1. Raman bands of the C=O stretching vibrations of propionic acid (parallel component): pure propionic acid (*1*); solutions of propionic acid in CCl_4 (*2, 3, 4, 5*), concentrations 0.7; 0.5; 0.3; 0.1, respectively. Intensities are not presented in the same scale

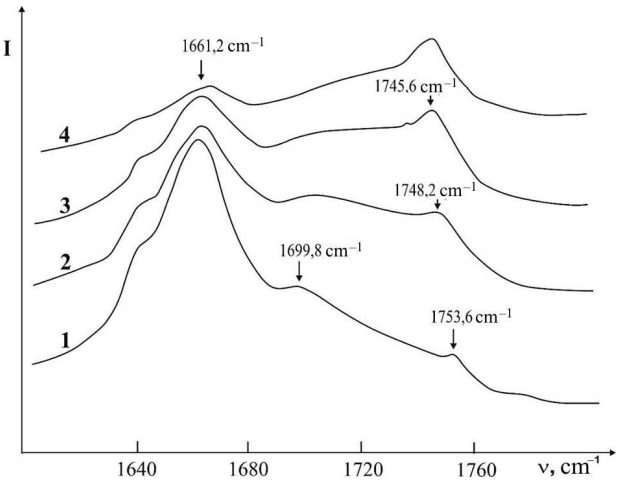

Fig. 2. Raman bands of the C=O stretching vibrations of propionic acid (parallel component): pure propionic acid (*1*); solutions of propionic acid in acetonitrile with concentrations 0.7 (*2, 3, 4*); 0.5; 0.3, respectively

should result in a different vibrational frequencies of the corresponding vibrations for different associates, as well as a difference in the derivatives of the anisotropy tensor and the coupling anisotropy tensor with respect to normal coordinates, resulting in a difference in the depolarization ratio. Thus, when the redistribution of the electron cloud during the formation of H-bonds leads to a change in the intensity of spectral bands in IR spectra, then, in Raman spectra, this distribution leads, first of all, to a change in the depolarization ratio of the band. This phenomenon can be explained by the fact that the C=O bond is partially ionic, so the bond strength (and the force constant) should be mainly determined by the residual charges on the C and O atoms.

So, the difference between frequencies of the C=O vibration in different complexes of PA can be explained by changes in the charge distribution on the atoms of the carboxylic group (COOH) at the hydrogen bonding formation. The 1753 cm^{-1} band is assigned to the C=O vibration in free molecules (monomers) of PA. During the formation of open dimers or longer chain complexes of PA molecules via the H-bond formation with the participation of the oxygen atom of the C=O group, a part of the electron cloud of this atom is attracted to the hydrogen of the O–H group of the neighbouring molecule. As a result, the residual negative charge on the oxygen atom decreases, the bond strength (force constant) of C and O atoms decreases, and, therefore, the frequency of the C=O vibration decreases. This means that the bands with lower frequencies can be assigned to PA associates.

In order to interpret each of the observed bands of the C=O stretching vibrations of propionic acid, the polarized Raman spectra of the solutions of propionic acid in CCl_4 were recorded. As one can see from Fig. 1, the ratio of the band intensities in PA solutions changes with concentration, but all three bands are observed at all concentrations. The band at 1661 cm^{-1} is the most intense one, and this tendency remains at all concentrations. So, one can conclude that the same associates of PA molecules exist both in pure PA and in the 10% solution in CCl_4.

In solutions of propionic acid in acetonitrile (AN), which is a strong proton acceptor, all three bands of C=O stretching vibrations are observed too (Fig. 2), but their intensity ratio changes with concentration. When the amount of acid in the solution is the least (30%), the relative intensity of the band with the highest frequency increases, while the maximum of the band shifts toward lower frequencies. The frequency of the band at 1661 cm^{-1} remains the same, but its intensity decreases with concentration deareasing. As a strong proton acceptor, AN forms a hydrogen bond with the hydrogen atom of the O–H group of propionic acid in the solution, resulting in

an increase in the number of the PA molecules with free C=O groups in the solution, and the relative intensity of the band corresponding to the free C=O group increases. The other observed bands of C=O vibrations can be assigned to PA dimers and bigger associates, as well as different complexes of PA with acetonitrile molecules.

Significant changes in the spectral region of the C=O stretching vibrations of propionic acid are observed in water solutions of PA with different concentrations (Fig. 3). In pure PA, the strongest band corresponds to the vibrations of PA associates. In the 70% solution, this band is still observed, but, already in the 50% solution, it almost disappears, and only one broad band at about 1720 cm^{-1} with some asymmetry on a low-frequency side is observed. With a further dilution, the situation remains the same, indicating the simultaneous presence of both PA associates and complexes of PA and water molecules.

3.2. Structural and vibrational analyses

Non-empirical calculations were carried out to properly explain and analyze the complexity of the polarized Raman spectra in the spectral region of the C=O stretching vibrations of propionic acid. Figure 4 shows the optimal geometric structures of propionic acid dimers calculated at the B3LYP/6-311++G(d,p) level of theory.

The calculations revealed that PA molecules form cyclic dimers with various mutual orientations via O–H···O and C–H···O hydrogen bonds. Dimer I, a cyclic structure formed by two O–H···O hydrogen bonds between carboxyl groups, is the most structurally and thermodynamically stable dimer of all considered structures (see Table 1). The following formula was used to calculate the intermolecular interaction energy (E_{int}) at the dimer formation:

$$E_{\text{int}} = E_{\text{dimer}} - 2\,E_{\text{monomer}}.$$

The calculated optimal geometry of a cyclic trimer of PA molecules is shown in Fig. 5. It is formed by three O–H···O hydrogen bonds between carboxyl groups.

From the data presented in Table 2, one can see that, in PA dimers (we will consider only the most stable structure – dimer I), the length of the C=O bond increases by 0.0215 Å compared to the monomer state. For the case of a trimer, this difference is 0.0133 Å. As a result, the corresponding vibrational frequency decreases by 60–110 cm^{-1} for the dimer and by 36–75 cm^{-1} for the trimer. These data can be used for the interpretation of the experimental spectra of PA, presented in Fig. 1. The band at 1753 cm^{-1} was assigned to the C=O vibrations in monomers. So, the band near 1700 cm^{-1} can belong to the corresponding vibrations in PA trimers, and the band at 1661 cm^{-1} – to PA dimers. Thus, PA dimers dominate both in pure acid and in its solutions in CCl_4.

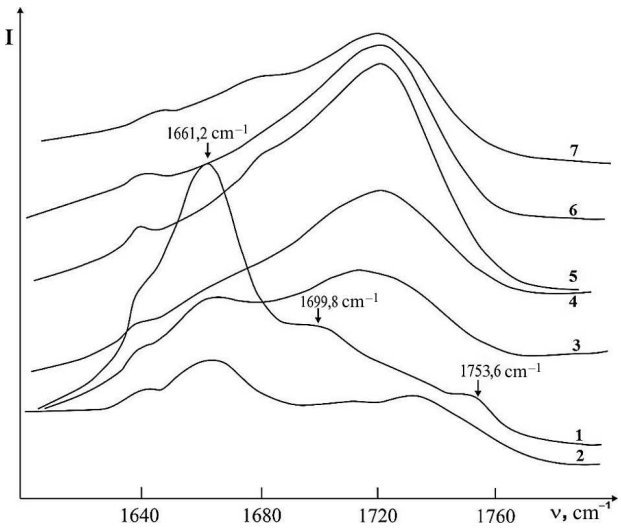

Fig. 3. Raman bands of the C=O stretching vibrations of PA: pure propionic acid (parallel and perpendicular components, respectively) (*1, 2*); solutions of PA in water with concentrations 0.7; 0.5; 0.3; 0.1; 0.05, respectively (*3, 4, 5, 6, 7*)

Figure 6 presents the results of geometry optimization for complexes consisting of PA with one or two acetonitrile molecules. In the case of one PA and one AN molecule the O–H···N hydrogen bond is formed. In the case of two AN molecules, they form a trimer with PA molecule via O–H···N, C–H···N and C–H···O hydrogen bonds. In the formation of PA + AN and PA + $(AN)_2$ complexes, the C=O bond length increases by 0.003 and 0.005 Å, respectively, compared to the PA monomer. The length of the O–H bond increases by 0.016 and 0.017 Å, respectively. The intermolecular interaction energies in PA + AN and PA + $(AN)_2$ complexes are 5.05 and 5.91 kcal/mol, respectively.

As can be seen from the calculation results, AN molecules in a solution form H-bonds with PA molecules. As a result, the amount of cyclic PA associates (dimer, trimer, *etc.*) is reduced. This causes

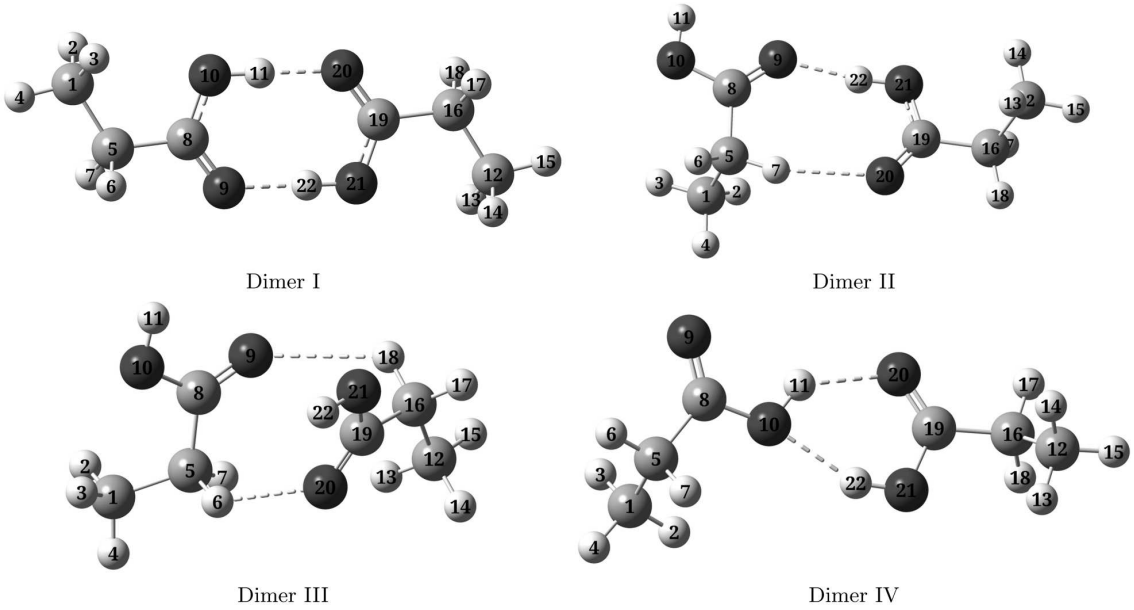

Dimer I Dimer II

Dimer III Dimer IV

Fig. 4. Optimal geometric structures of PA dimers. Red, gray, and white balls represent oxygen, carbon, and hydrogen atoms, respectively

Table 1. **Calculated parameters of PA dimers**

Dimer	Energy E, Hartree	Relative energy ΔE, kcal/mol	Interaction energy E_{int}, kcal/mol	Gibbs free energy G, a.u.	Dipole moment D, Debye
Dimer I	–537.0011	0	16.41	0.1445	0.0138
Dimer II	–536.9896	7.22	9.19	0.1381	1.3964
Dimer III	–536.9809	7.59	3.77	0.1334	0.7191
Dimer IV	–536.9878	8.34	8.07	0.1381	3.6961

Table 2. **Calculated C=O bond lengths and the corresponding vibrational frequencies of PA molecular associates**

PA molecular associates	Bond length $r_{\text{C=O}}$, Å	Frequency $\nu_{\text{C=O}}$, cm^{-1}
Monomer	1.2063	1804.78
Dimer	1.2278	1745.61
	1.2278	1693.05
Trimer	1.2196	1768.67
	1.2196	1768.54
	1.2196	1729.86

a decrease in the relative intensity of the Raman bands of the C=O stretching vibrations near 1661 and 1700 cm^{-1} assigned to PA dimers and trimers, respectively (see Fig. 2).

Figure 7 shows that, at the formation of PA + AN and PA + $(AN)_2$ complexes, the C=O vibrational frequency of PA decreases by 14 and 19 cm^{-1}, respectively. This fact explains the low-frequency shift of the band near 1753 cm^{-1} with dilution of propionic acid with acetonitrile (see Fig. 2).

The calculated optimal structures of PA molecules with different numbers of water molecules are presented in Fig. 8. The calculated energies and dipole moments of the corresponding complexes are presented in Table 3. The intermolecular interaction energies in complexes were determined using the following formula:

$$E_{\text{int}} = E_{\text{complex}} - (E_{\text{monomer}} + n\,E_{\text{water}}).$$

When water molecules interact with PA, the carboxyl group of PA serves both as a donor and an accep-

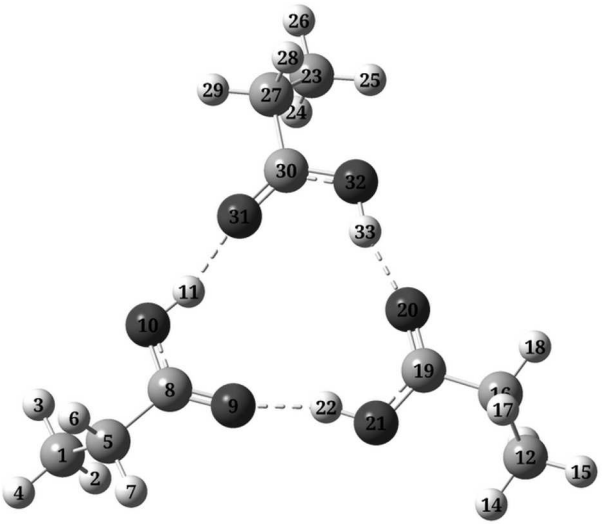

Fig. 5. Optimal geometric structure of a PA trimer

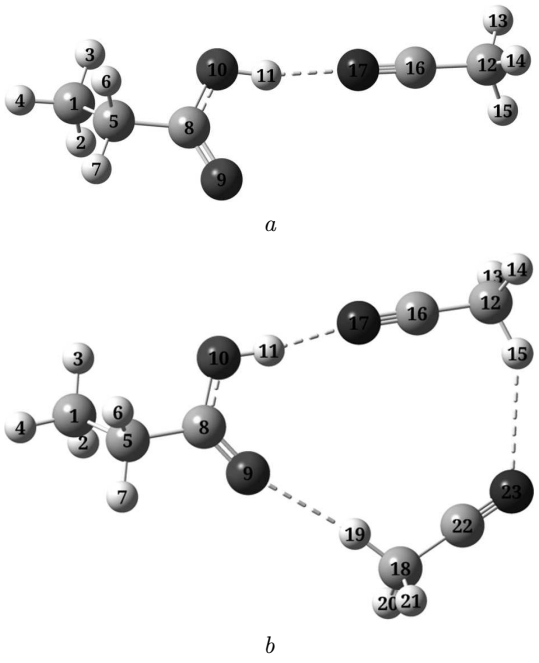

Fig. 6. Optimal geometric structures of PA + AN (*a*) and PA + $(AN)_2$ (*b*) complexes. Gray, white, red, and blue balls represent carbon, hydrogen, oxygen, and nitrogen atoms, respectively

tor in the H-bond formation. PA molecules can form cyclic structures with one to three water molecules via O–H···O hydrogen bonds (Fig. 8, *a*–*c*). With four or five water molecules, the PA molecule forms bicyclic complexes (Fig. 8, *d*–*e*). Six water molecules

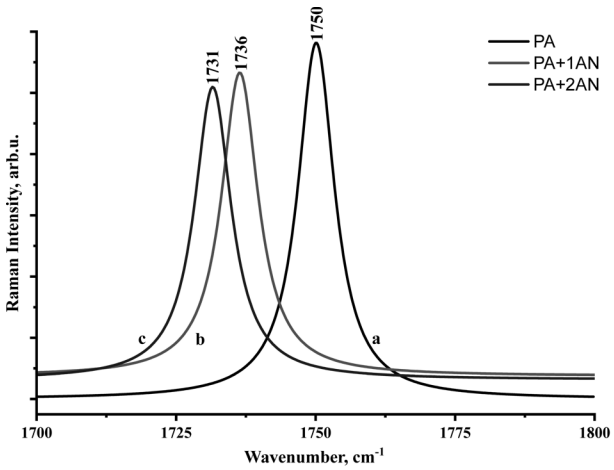

Fig. 7. Calculated Raman frequencies of the C=O stretching vibrations of PA molecule (*a*), PA + AN (*b*) and PA + $(AN)_2$ (*c*) complexes

Table 3. **Some calculated parameters of complexes PA + W_n (n = 1–6)**

Complexes	Total energy E, Hartree	Intermolecular interaction energy E_{int}, kcal/mol	Dipole momentum D, Debye
PA + W1	–344.971484	6.13	1.907923
PA + W2	–421.451032	14.33	3.225948
PA + W3	–497.927415	20.55	1.122380
PA + W4	–574.399949	24.35	3.962489
PA + W5	–650.877274	31.15	6.301351
PA + W6	–727.349233	34.60	6.396253

form a triple cyclic structure with the PA molecule (Fig. 8, *f*). The increase of the number of water molecules per one PA molecule leads to the formation of chain-like clusters with mutual hydrogen bonds.

The calculated Raman spectra of PA + W_n complexes in the spectral region of the stretching C=O vibrations are presented in Fig. 9. It is seen that when the PA molecule interacts with water molecules, the band of the C=O stretching vibrations shifts toward lower frequencies. The observed shift is from 20 cm^{-1} for the complexes with one and five water molecules to 45 cm^{-1} for 2 and 3 water molecules. The additional bands observed in the region 1600–1700 cm^{-1} belong to the O–H bending vibrations of water molecules in these complexes [33]. So, the broad band observed in the Raman spectra of PA solutions in wa-

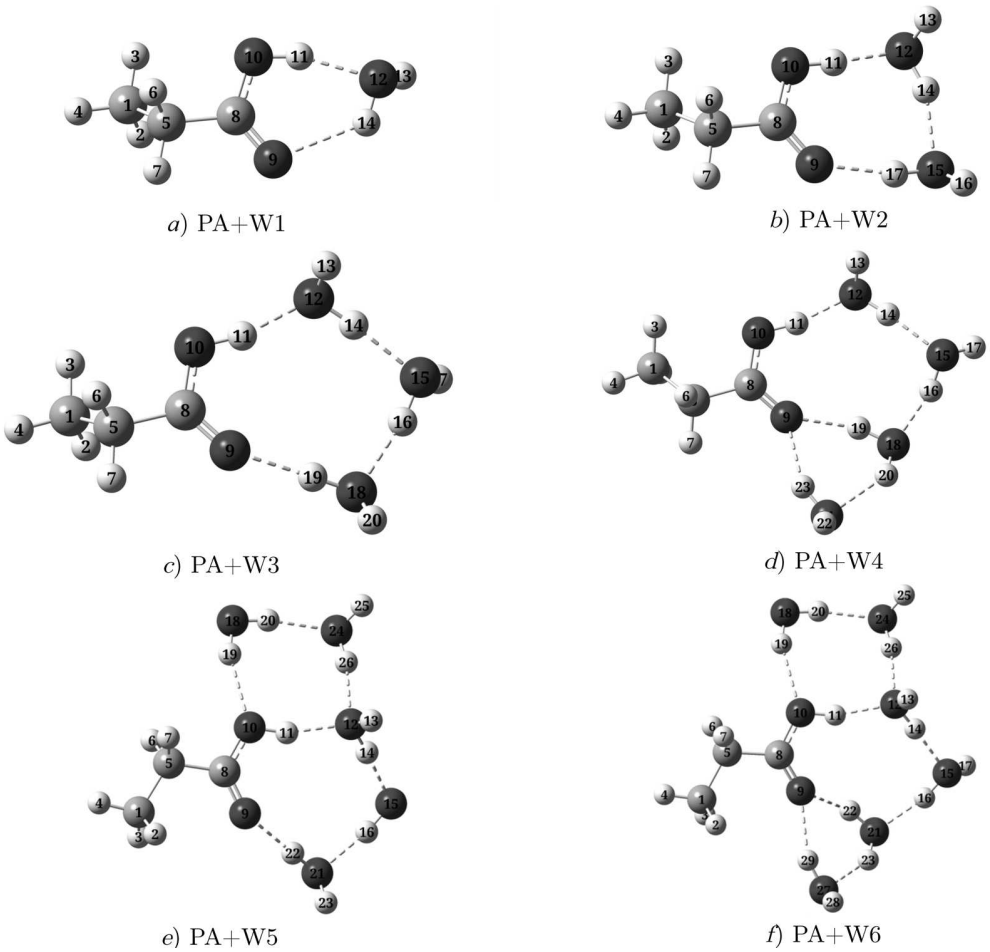

a) PA+W1 *b*) PA+W2 *c*) PA+W3 *d*) PA+W4 *e*) PA+W5 *f*) PA+W6

Fig. 8. Optimal geometrical structures of complexes of PA with water molecules. Gray, white, and red balls represent carbon, hydrogen, and oxygen atoms, respectively

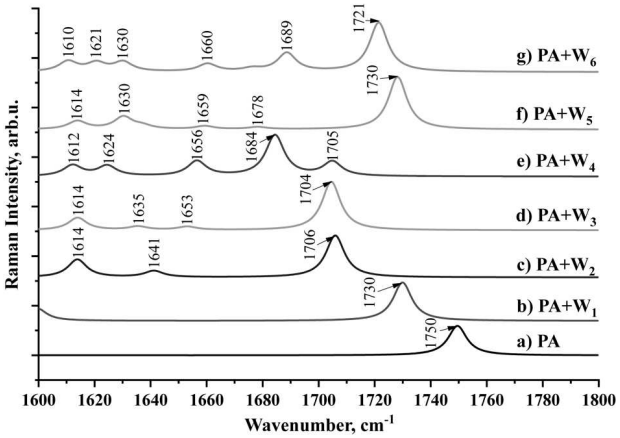

Fig. 9. Calculated Raman frequencies of the C=O stretching vibrations of $PA + W_n$ complexes

ter near 1720 cm^{-1} can be assigned to $PA + W_n$ complexes.

3.3. AIM, RDG and NCI topological analysis

The topological electron density analysis is an effective method for investigating the nature of intermolecular hydrogen bonds in molecular complexes [34–36]. According to [37], the strength of hydrogen bond can be described using such topological parameters as the electron density $\rho(r)$ and energy density H(r) as follows:

- $\nabla^2\rho(r) > 0$, $H(r) > 0$ and $E_{HB} < 12$ kcal/mol – weak hydrogen bonding;
- $\nabla^2\rho(r) > 0$, $H(r) < 0$ and $12 < E_{HB} < 24$ kcal/mol – medium hydrogen bonding;

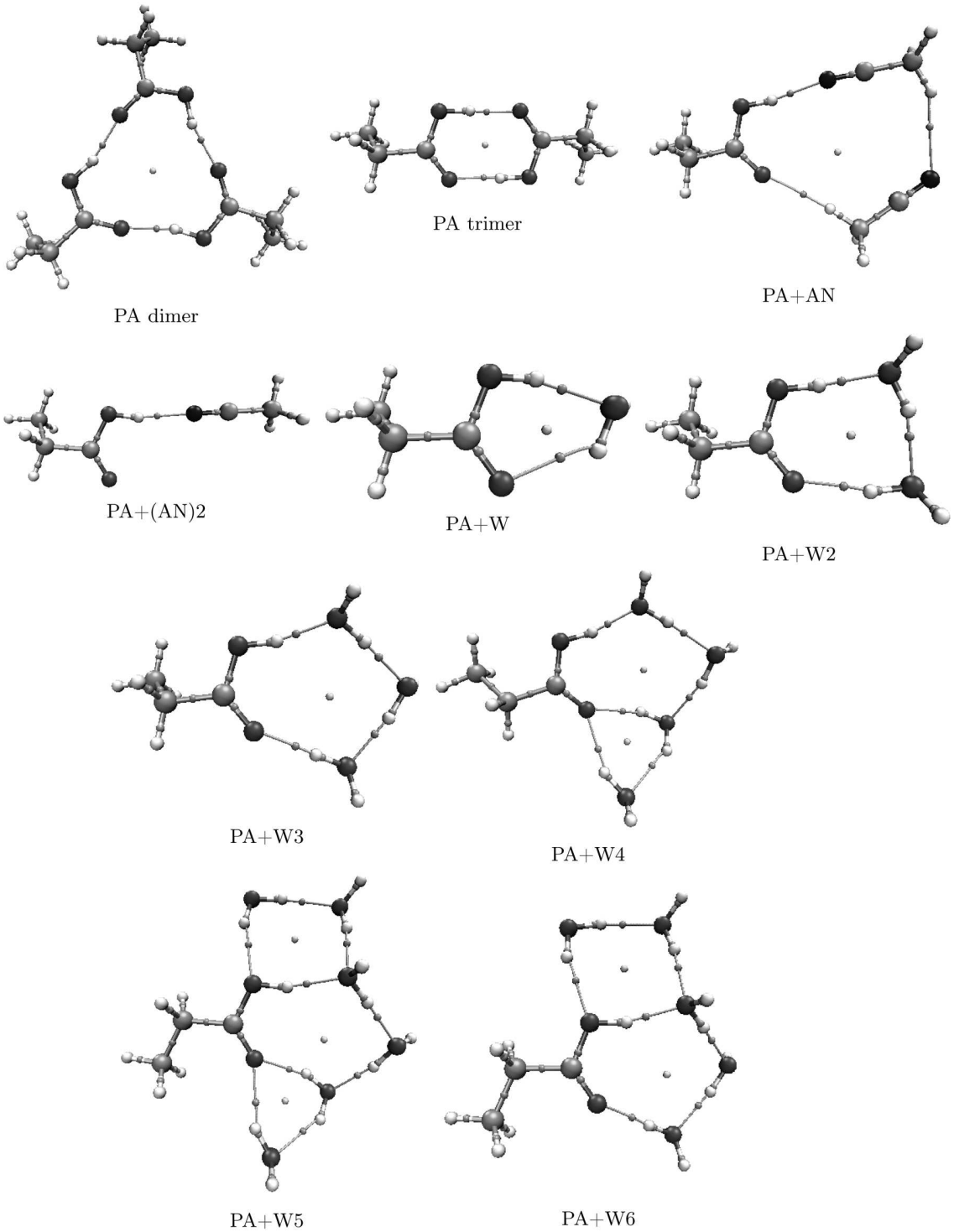

Fig. 10. AIM molecular graph showing different BCPs of a PA dimer, trimer, $PA + (AN)_n$, and $PA + W_n$ complexes calculated at the B3LYP/6-311++G(d, p) level. The critical points of H-bonds are indicated by small orange balls

Table 4. **Topological parameters at the BCP of the complexes**

Complex	BCP	Electron density, $\rho(r_{\mathrm{BCP}})$	Laplacian of electron density, $\nabla^2\rho(r_{\mathrm{BCP}})$	Energy density, $H(r_{\mathrm{BCP}})$	Potential energy density, $V(r_{\mathrm{BCP}})$	H-bond energy, E_{int}
PA dimer	O10–H11 ... O20	0.0462	0.1351	–0.0047	–0.0431	13.52
	O21–H22 ... O9	0.0462	0.1351	–0.0047	–0.0431	13.52
PA trimer	O10–H11 ... O31	0.0351	0.1367	0.0009	–0.0324	10.16
	O21–H22 ... O9	0.0348	0.1363	0.0010	–0.0321	10.07
	O32–H33 ... O20	0.0348	0.1365	0.0010	–0.0321	10.07
PA + AN	O10–H11 ... N17	0.0323	0.0989	–0.0001	–0.0250	7.84
PA + (AN)2	O10–H11 ... N17	0.0335	0.1005	–0.0006	–0.0263	8.25
	C18–H19 ... N9	0.0097	0.0343	0.0014	–0.0057	1.78
	C12–H15 ... N23	0.0072	0.0212	0.0009	–0.0035	1.10
PA + W	O10–H11 ... O12	0.0390	0.1228	–0.0017	–0.0342	10.73
	O12–H14 ... O9	0.0166	0.0571	0.0014	–0.0114	3.58
PA + W2	O10–H11 ... O12	0.0477	0.1343	–0.0055	–0.0446	13.99
	O12–H14 ... O15	0.0362	0.1203	–0.0005	–0.0311	9.76
	O15–H17 ... O9	0.0309	0.1125	0.0014	–0.0254	7.94
PA + W3	O10–H11 ... O12	0.0483	0.1390	–0.0055	–0.0461	1446
	O12–H14 ... O15	0.0408	0.1285	–0.0022	–0.0366	11.48
	O15–H16 ... O18	0.0388	0.1275	–0.0012	–0.0344	10.79
	O18–H19 ... O9	0.0303	0.1188	0.0020	–0.0256	8.03
PA + W4	O10–H11 ... O12	0.0488	0.1296	–0.0058	–0.0466	14.62
	O12–H14 ... O15	0.0392	0.1242	–0.0016	–0.0344	10.79
	O15–H16 ... O18	0.0382	0.1245	–0.0011	–0.0334	10.48
	O18–H19 ... O9	0.0240	0.0938	0.0025	–0.0185	5.80
	O21–H23 ... O9	0.0223	0.0877	0.0026	–0.0166	5.21
	O18–H20 ... O21	0.0217	0.0761	0.0016	–0.0157	4.92
PA + W5	O18–H20 ... O24	0.0290	0.1014	0.0013	–0.0228	7.15
	O18–H19 ... O10	0.0172	0.0647	0.0022	–0.0117	3.67
	O24–H26 ... O12	0.0298	0.1054	0.0013	–0.0238	7.47
	O10–H11 ... O12	0.0423	0.1283	–0.0031	–0.0382	1198
	O12–H14 ... O15	0.0456	0.1360	–0.0043	–0.0425	13.33
	O21–H22 ... O9	0.0287	0.1140	0.0024	–0.0237	7.43
	O15–H16 ... O21	0.0391	0.1278	–0.0014	–0.0347	10.89
PA + W6	O18–H19 ... O10	0.0160	0.0594	0.0021	–0.0106	3.32
	O18–H20 ... O24	0.0146	0.1021	0.0012	–0.0230	7.22
	O24–H26 ... O12	0.0299	0.1057	0.0012	–0.0239	7.50
	O27–H29 ... O9	0.0191	0.0785	0.0029	–0.0138	4.33
	O21–H22 ... O9	0.0218	0.0848	0.0025	–0.0162	5.08
	O21–H23 ... O27	0.0232	0.0814	0.0016	–0.0172	5.40
	O15–H16 ... O21	0.0393	0.1262	–0.0016	–0.0348	10.92
	O10–H11 ... O12	0.0418	0.1272	–0.0029	–0.0376	1180
	O12–H14 ... O15	0.0446	0.1337	–0.0039	–0.0412	12.93

• $\nabla^2\rho(r) < 0$, $H(r) < 0$ and 24 kcal/mol $< E_{\mathrm{HB}} <$ – strong hydrogen bonding.

The molecular diagram of a PA dimer, trimer, $\mathrm{PA} + (\mathrm{AN})_{n=1-2}$ and $\mathrm{PA} + \mathrm{W}_{n=1-6}$ complexes is shown in Fig. 10. Topological parameters at the bond critical point (BCP) such as the electron density $\rho(r_{\mathrm{CP}})$, Laplacian of the electron density $\nabla^2\rho(r_{\mathrm{CP}})$, energy density $H(r_{\mathrm{CP}})$, potential energy density $V(r_{\mathrm{CP}})$, and hydrogen bond energy E_{HB} were calculated at the B3LYP/6-311++G(d,p) level (Table 4).

The calculation results show that the electron density values at the bond critical points are of 0.046 a.u.

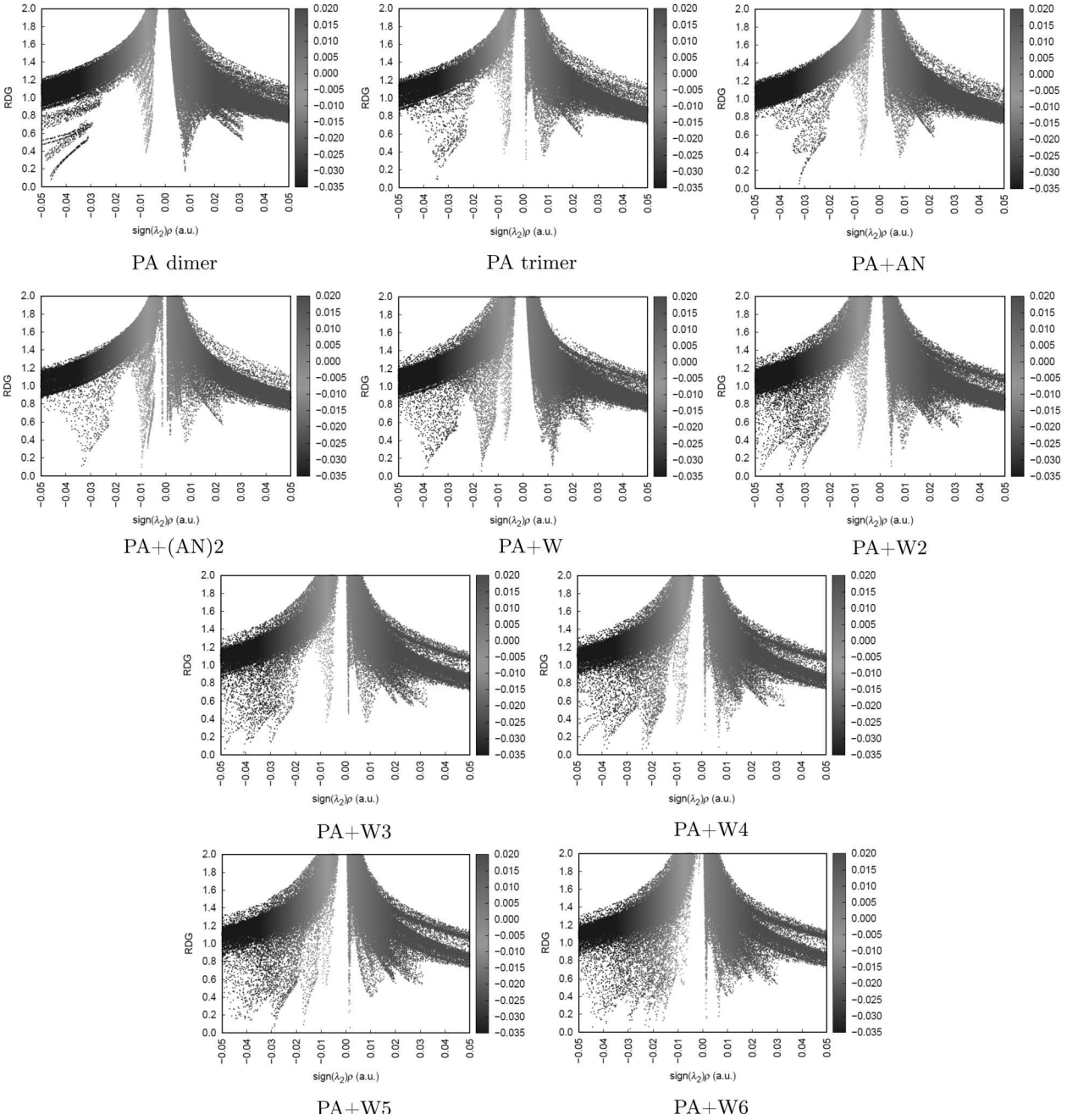

Fig. 11. RDG analysis of complexes

and 0.035 a.u. for PA dimer and trimer, respectively. For $\mathrm{PA}+(\mathrm{AN})_{n=1-2}$ and $\mathrm{PA}+\mathrm{W}_{n=1-6}$ complexes, these values are in the interval from 0.007 to 0.032 a.u. Thus, all these values fall into the hydrogen bond interval (0.003–0.168 a.u.) [38, 39]. The electron density Laplacian ($\nabla^2\rho_{\mathrm{BCP}}$) values lie between 0.135 a.u. and 0.137 a.u. for PA dimer and trimer. For complexes $\mathrm{PA}+(\mathrm{AN})_{n=1-2}$ and $\mathrm{PA}+\mathrm{W}_{n=1-6}$, this value is between 0.02 a.u. and 0.013 a.u. All of them are in the interval of the hydrogen bonding

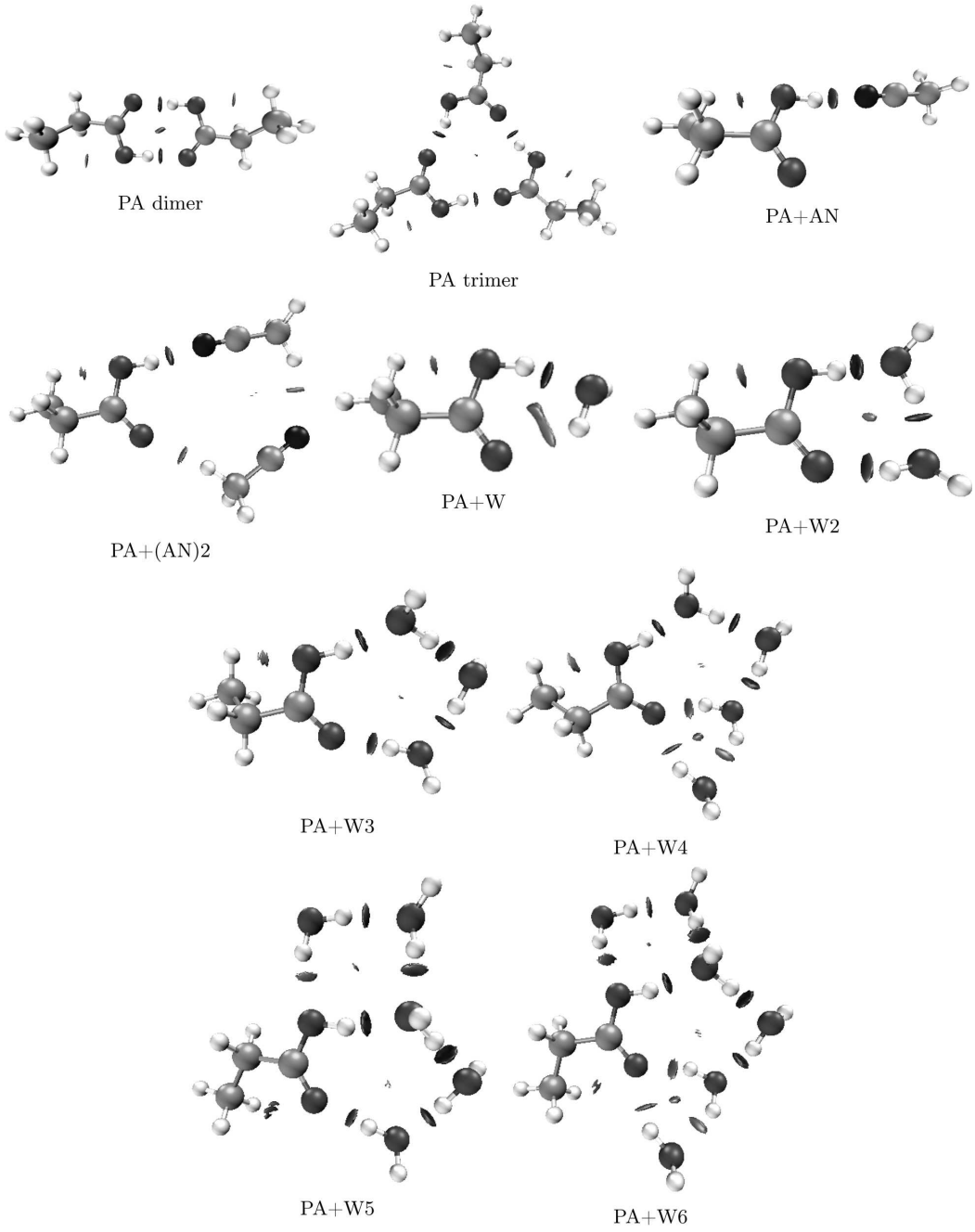

Fig. 12. NCI analysis of complexes

(0.024–0.139 a.u.) [38, 39], thus confirming the presence of the hydrogen bonding in the complex.

The hydrogen bond energy was determined using the formula [40]:

$E_{\mathrm{HB}} = -V(r_{\mathrm{CP}})\,627.5/2.$

Here, $V(r_{\mathrm{CP}})$ is the potential energy density at the critical points of hydrogen bonding.

If the value of the energy density at the critical point is negative ($H_{\mathrm{BCP}} < 0$), the hydrogen bond has a covalent character, and if it is positive ($H_{\mathrm{BCP}} > 0$),

it has an electrostatic character [35, 41]. It can be seen that the covalent effect is dominant in the O–H···O H-bonds in the PA dimer, and the electrostatic effect is dominant in the O–H···O H-bonds in the PA trimer. Thus, the hydrogen bond energy in the PA dimer is ≈13.5 kcal/mol, and the hydrogen bond energy in the trimer is ≈10 kcal/mol. In the PA + AN and PA + $(AN)_2$ complexes, the covalent effect is dominant in the O–H···N H-bonds, and the electrostatic effect is dominant in the C–H···N H-bonds. PA + W_n complexes are formed via H-bonds with an energy of 3.32–14.62 kcal/mol.

The non-covalent interaction (NCI) index is used to describe intermolecular interactions and assess the nature of weak interactions. The NCI index is based on the reduced density gradient (RDG) and provides more evidence for non-covalent interactions [34–41]. The reduced density gradient (RDG) is a basic dimensionless quantity consisting of the density and its first derivative expressed using the following relation [42]:

$$\mathrm{RDG}\,(r) = \frac{1}{2(3\pi^2)^{1/3}} \frac{|\nabla\rho(r)|}{\rho(r)^{4/3}}.$$

The quantification of the electron density of the sign $(\lambda_2)\rho$ peaks relative to RDG gives us information about the nature and strength of the molecular interactions. In the molecular system, blue represents attractive interaction and red represents repulsive interaction. The sign $(\lambda_2)\rho$ value is critical in predicting the nature of the interaction; for example, sign $(\lambda_2)\rho < 0$ indicates a repulsive interaction (bonded), while sign $(\lambda_2)\rho > 0$ and the symbol indicate a repulsive interaction (not connected). The RDG scatter graphs of the complexes are shown on Fig. 11. Red color is defined as strong repulsion (steric effect), blue represents hydrogen bonding interactions, and green represents van der Waals interactions. As can be seen on Fig. 12, the blue color indicates the hydrogen bonding, the green color corresponds to the van der Waals interaction, and the red color corresponds to the steric or cyclic effect. The results show that, in the formation of molecular complexes, O–H···O bonds are represented by blue disks, which correspond to strong hydrogen bonds. C–H···O bonds are represented by blue-green disks, which show weak hydrogen bonds.

4. Conclusions

In the experimentally registered Raman spectra of pure liquid propionic acid, the band of the stretching C=O vibrations is complex. This complexity is explained by the presence of various associates of PA molecules in the liquid. The Raman and DFT studies of PA solutions in CCl_4 and acetonitrile allowed making a more accurate interpretation of the components of the C=O vibrational band.

In aqueous solutions of propionic acid, the strong hydrogen bonds are formed between PA and water molecules. As a result, the shape of the C=O vibrational band in this solution changes radically.

Quantum-chemical calculations of the optimal geometric structures and interaction energies of four dimers of PA are made using the DFT approach and the B3LYP/6-311++G(d,p) basis set, and the most stable dimer is determined. At the same level of theory, the corresponding calculations for a PA trimer, PA + $(AN)_1$, PA + $(AN)_2$, and PA + W_n (n = 1–6) complexes are carried out. The Raman spectra of all considered complexes in the spectral region of the C=O stretching vibrations are calculated, and the effect of the intermolecular hydrogen bonding on the formation of a complex is estimated.

The AIM, RDG, and NCI topological analyzes confirmed that the intermtheolecular hydrogen bonding plays a dominant role in the formation of complexes.

This work is supported by the Ministry of Innovative Development of the Republic of Uzbekistan in the frame of the State scientific and technical program for fundamental research, project No. FZ-20200929385, Samarkand State University, Uzbekistan.

1. R.J. Jakobsen, Y. Mikawa, J.W. Brasch. Far infrared studies of hydrogen bonding in carboxylic acids – I. Formic and acetic acids. *Spectrochim. Acta A* **23** (7), 2199 (1967).
2. K. Nakamoto, S. Kishida. Normal coordinate analyses of hydrogen-bonded compounds. I. Monomeric formic acid and acetic acid. *J. Chem. Phys.* **41** (6), 1554 (1964).
3. L.J. Bellamy, R.J. Pace. Hydrogen bonding in carboxylic acids – I. Oxalic acids. *Spectrochim. Acta* **19** (2), 435 (1963).
4. R.J. Jakobsen, Y. Mikawa, J.W. Brasch. Far infrared studies of hydrogen bonding in carboxylic acids – II. The n-alkyl acids, propanoic to undecanoic. *Spectrochim. Acta A 25* (4), 839 (1969).
5. K.A.E. Meyer, A. Nejad. CC-stretched formic acid: Isomerisation, dimerisation, and carboxylic acid complexation. *Phys. Chem. Chem. Phys.* **23** (32), 17208 (2021).
6. K.A.E. Meyer, M.A. Suhm. Vibrational exciton coupling in homo and hetero dimers of carboxylic acids studied by linear infrared and raman jet spectroscopy. *J. Chem. Phys.* **149** (10), 104307 (2018).

7. T.Yu. Nikolaenko, L.A. Bulavin, D.N. Govoruna. Quantum mechanical interpretation of the IR Spectrum of 2-deoxy-D-ribose in the oh group stretching vibration region. *J. Appl. Spectr.* **78** (5), 751 (2011).
8. P. Excoffon, Y. Marechal. Infrared spectra of H-bonded systems: Saturated carboxylic acid dimers. *Spectrochim. Acta A* **28** (2), 269 (1972).
9. M. Faubel, Th. Kisters. Non-equilibrium molecular evaporation of carboxylic acid dimers. *Nature* **339** (6225), 527 (1989).
10. J. Chen, Ch.L. Brooks, 3rd, H.A. Scheraga. Revisiting the carboxylic acid dimers in aqueous solution: Interplay of hydrogen bonding, hydrophobic interactions, and entropy. *J. Phys. Chem. B* **112** (2), 242 (2008).
11. G.M. Florio, T.S. Zwier, E.M. Myshakin, K.D. Jordan, E.L. Sibert. III. Theoretical modeling of the oh stretch infrared spectrum of carboxylic acid dimers based on first-principles anharmonic couplings. *J. Chem. Phys.* **118** (4), 1735 (2003).
12. C. Colominas, J. Teixido, J. Cemeli, F.J. Luque, M. Orozco. Dimerization of carboxylic acids: Reliability of theoretical calculations and the effect of solvent. *J. Phys. Chem. B* **102** (12), 2269 (1998).
13. A. Jumabaev, U. Holikulov, H. Hushvaktov, A. Absanov, L. Bulavin. Interaction of valine with water molecules: Raman and dft study. *Ukr. J. Phys.* **67** (8), 602 (2022).
14. M.Kh. Khodiev, U.A. Holikulov, N. Issaoui, O.M. Al-Dossary, L.G. Bousiakoug, N.L. Lavrik. Estimation of electrostatic and covalent contributions to the enthalpy of h-bond formation in h-complexes of 1,2,3-benzotriazole with proton-acceptor molecules by IR spectroscopy and DFT calculations. *J. King Saud Univ. Sci.* **35** (3), 102530 (2023).
15. G.A. Pitsevich, A.E. Malevich, E.N. Kozlovskaya, I.Yu. Doroshenko, V. Sablinskas, V.E. Pogorelov, D. Dovgal, V. Balevicius. Anharmonic analysis of CH and OH stretching vibrations of the formic acid dimer. *Vib. Spectrosc.* **79**, 67 (2015).
16. R. Kalescky, E. Kraka, D. Cremer. Accurate determination of the binding energy of the formic acid dimer: The importance of geometry relaxation. *J. Chem. Phys.* **140** (8), 084315 (2014).
17. K.G. Goroya, Yu. Zhu, P. Sun, Ch. Duan. High resolution jet-cooled infrared absorption spectra of the formic acid dimer: A reinvestigation of the C–O stretch region. *J. Chem. Phys.* **140** (16), 164311 (2014).
18. W. Qian, S. Krimm. Origin of the CO stretch mode splitting in the formic acid dimer. *J. Phys. Chem.* **100** (35), 14602 (1996).
19. J. Dybal, T.C. Cheam, S. Krimm. C=O stretch mode splitting in the formic acid dimer: Electrostatic models of the intermonomer interaction. *J. Mol. Struct.* **159** (1–2), 183 (1987).
20. F. Bardak, C. Karaca, S. Bilgili, A. Atac, T. Mavis, A.M. Asiri, M. Karabacak, E. Kose. Conformational, electronic, and spectroscopic characterization of isophthalic acid (monomer and dimer structures) experimentally and by DFT. *Spectrochim. Acta A Mol. Biomol. Spectrosc.* **165**, 33 (2016).
21. H.H. Pham, Ch.D. Taylor, N.J. Henson. First-principles prediction of the effects of temperature and solvent selection on the dimerization of benzoic acid. *J. Phys. Chem. B* **117** (3), 868 (2013).
22. N. Martsinovich, A. Troisi. Modeling the self-assembly of benzenedicarboxylic acids using monte carlo and molecular dynamics simulations. *J. Phys. Chem. C Nanomater. Interfaces* **114** (10), 4376 (2010).
23. R. Alcala, S. Martínez-Carrera. The crystal structure of isophthalic acid. *Acta Crystallogr. B* **28** (6), 1671 (1972).
24. J.L. Derissen. The crystal structure of isophthalic acid. *Acta Crystallogr. B* **30** (11), 2764 (1974).
25. Jin-Ling Mi, Le Chen, Ming-Yang He. 5-fluoro-isophthalic acid. *Acta Crystallogr. Sect. E Struct. Rep. Online* **67** (3), o590 (2011).
26. F.H. Tukhvatullin, U.N. Tashkenbaev, A. Jumaboev, S.A. Osmanov, Z.U. Mamatov, H.A. Hushvaktov. The shape of different polarized components of 1710 cm^{-1} raman band for methyl ethyl ketone (2-butanone) and its solutions. *Ukr. J. Phys.* **46** (9), 922 (2001).
27. Th. Gomti Devi, Ganesh Upadhayay. Solvent dependent raman bandshape analysis on CO containing molecules: Vibrational relaxation study. *Spectrochim. Acta A Mol. Biomol. Spectrosc.* **91**, 106 (2012).
28. M.J. Frisch, G.W. Trucks, H.B. Schlegel *et al.* Gaussian 09, 2009. Gaussian Inc. Wallingford CT.
29. R.F.W. Bader. Atoms in molecules. *Acc. Chem. Res.* **18** (1), 9 (1985).
30. T.Yu. Nikolaienko, E.S. Kryachko, G.A. Dolgonos. On the existence of He–He bond in the endohedral fullerene $He_2@C_{60}$. *J. Computational Chem.* **39** (18), 1090 (2018).
31. T.Yu. Nikolaienko, E.S. Kryachko. Formation of dimers of light noble atoms under encapsulation within fullerene's voids. *Nanoscale Res. Lett.* **10** (1), 185 (2015).
32. E.S. Kryachko, T.Yu. Nikolaienko. $He_2@C_{60}$: Thoughts of the concept of a molecule and of the concept of a bond in quantum chemistry. *Intern. J. Quantum Chem.* **115** (14), 859 (2015).
33. Tian Lu, Feiwu Chen. Multiwfn: A multifunctional wavefunction analyzer. *J. Comput. Chem.* **33** (5), 580 (2012).
34. W. Humphrey, A. Dalke, K. Schulten. VMD: Visual molecular dynamics. *J. Mol. Graph.* **14** (1), 33 (1996).
35. Th. Gomti Devi, Bhargab Borah. Non-coincidence effect study of NN-Dibutyl formamide in binary liquid mixtures. *J. Mol. Liq.* **309**, 113174 (2020).
36. Kh. Khushvaktov, A. Jumabaev, V. Pogorelov, U. Tashkenbaev, A. Absanov, G. Sharifov, B. Amrullaeva. Intermolecular hydrogen bond in acetic acid solutions. Raman spectra and ab initio calculations. *American J. Phys. Appl.* **6** (6), 169 (2019).
37. E.N. Kozlovskaya, G.A. Pitsevich, A.E. Malevich, O.P. Doroshenko, V.E. Pogorelov, I.Yu. Doroshenko, V. Balevicius,

V. Sablinskas, A.A. Kamnev. Raman spectroscopic and theoretical study of liquid and solid water within the spectral region 1600–2300 cm^{-1}. *Spectrochim. Acta A Mol. Biomol. Spectrosc.* **196**, 406 (2018).
38. R.F.W. Bader. A quantum theory of molecular structure and its applications. *Chem. Rev.* **91** (5), 893 (1991).
39. N. Chetry, Th. Gomti Devi. Intermolecular interaction study of l-threonine in polar aprotic solvent: Experimental and theoretical study. *J. Mol. Liq.* **338**, 116689 (2021).
40. Sh.S. Malaganvi, J.T. Yenagi, J. Tonannavar. Experimental, DFT dimeric modeling and AIM study of H-bond-mediated composite vibrational structure of Chelidonic acid. *Heliyon* **5** (5), e01586 (2019).
41. I. Rozas, I. Alkorta, J. Elguero. Behavior of ylides containing N, O, and C atoms as hydrogen bond acceptors. *J. Am. Chem. Soc.* **122** (45), 11154 (2000).
42. H. Roohi, A.-R. Nowroozi, E. Anjomshoa. H-bonded complexes of uracil with parent nitrosamine: A quantum chemical study. *Comput. Theor. Chem.* **965** (1), 211 (2011).
43. T-H. Tang, E. Deretey, S.J. Knak Jensen, I.G. Csizmadia. Hydrogen bonds: Relation between lengths and electron densities at bond critical points. *Eur. Phys. J. D* **37** (2), 217 (2006).
44. E. Espinosa, E. Molins, C. Lecomte. Hydrogen bond strengths revealed by topological analyses of experimentally observed electron densities. *Chem. Phys. Lett.* **285** (3–4), 170 (1998).
45. L.F. Pacios. Topological descriptors of the electron density and the electron localization function in hydrogen bond dimers at short intermonomer distances. *J. Phys. Chem. A* **108** (7), 1177 (2004).
46. N.S. Venkataramanan, A. Suvitha. Nature of bonding and cooperativity in linear DMSO clusters: A DFT, AIM and NCI analysis. *J. Mol. Graph. Model.* **81**, 50 (2018).

Received 20.05.23

А. Жумабаєв, А.А. Абсанов,
Х.А. Хушвактов, Л.А. Булавін

МІЖМОЛЕКУЛЯРНІ ВЗАЄМОДІЇ В РІДКІЙ ПРОПІОНОВІЙ КИСЛОТІ ТА ЇЇ РОЗЧИНАХ: ДОСЛІДЖЕННЯ ЗА ДОПОМОГОЮ РАМАНІВСЬКОЇ СПЕКТРОСКОПІЇ ТА ТЕОРІЇ ФУНКЦІОНАЛА ГУСТИНИ

Досліджено механізм утворення молекулярних комплексів у рідкій пропіоновій кислоті та її розчинах. Анізотропна складова смуги комбінаційного розсіювання валентних коливань C=O чистої пропіонової кислоти складається з трьох смуг з максимумами при 1661, 1700 і 1753 $см^{-1}$. Було досліджено вплив різних концентрацій розчинників, таких як CCl_4, ацетонітрил і вода, на вказані коливання. Механізм утворення молекулярних комплексів у розчинах досліджено за допомогою розрахунків DFT на рівні теорії B3LYP/6-311++G(d, p). Проведено топологічний аналіз методами AIM, RDG і NCI для дослідження міжмолекулярних взаємодій у комплексах.

Ключові слова: пропіонова кислота, раманівська спектроскопія, теорія функціонала густини, міжмолекулярні взаємодії.